Global and Stochastic Analysis
Vol. 8 No. 3 (December, 2021)
Special Issue: Modern Stochastic Models and Problems of Actuarial Mathematics

ITERATED LOGARITHM BOUNDS OF BI-DIRECTIONAL GRID CONSTRAINED STOCHASTIC PROCESSES

ALDO TARANTO, SHAHJAHAN KHAN, RON ADDIE

Abstract. We derive a novel framework called Bi-Directional Grid Constrained (BGC) stochastic processes in which the further an Itô diffusion drifts away from the origin, then the further it will be constrained. By making suitable modifications to the Law of Iterated Logarithm (LIL), we derive a novel theorem about the upper and lower bounds for BGC processes and their hidden barrier. To visualize the theorem, we run many simulations of the Itô diffusions for a representative expression for $\lambda(X,t)$, both before and after BGC and uncover some interesting results with applications into finance and many other areas.

1. Introduction

The problem that this paper solves is the identification of a novel class of Itô diffusions and their corresponding formulation, in which the further they drift away from the origin, then the more resistence and hence constraining they undergo. We examine the constraining of stochastic processes by subtle perturbations rather than by the usual direct perturbations, such as through the use of hard barriers. One of the earliest forms of subtle constraining is the Langevin equation of Physics (Langevin, 1908) [12]. The Langevin equation is a stochastic differential equation (SDE) that describes a particular form of Brownian motion, the apparently random movement of a particle in a fluid due to its collisions with other particles in the fluid and is expressed as,

$$m\,\frac{d\mathbf{v}}{dt} \quad = \quad \underbrace{\boldsymbol{\eta}\,(t)}_{\text{stochastic term}} \quad - \quad \underbrace{\lambda\mathbf{v}}_{\text{constraining term}} \quad ,$$

where m is the mass of the particle, $\mathbf{v}$ is its velocity and t is time. The force acting on the particle is written as a sum of a viscous force proportional to the particle's velocity (Stokes' law), and a noise term $\boldsymbol{\eta}\,(t)$, noting that $\mathbf{v}$ and $\boldsymbol{\eta}$ are vectors. If the random $\boldsymbol{\eta}\,(t)$ term was not present, then the above equation would simply

---

E-mail address: `Aldo.Taranto@, Shahjahan.Khan@, Ron.Addie@, @usq.edu.au`.

2000 *Mathematics Subject Classification.* Primary 60G40; Secondary 60J60, 65R20, 60J65.

Key words and phrases. Wiener Process, Itô Processes, Law of Iterated Logarithm (LIL), Bi-Directional Grid Constrained (BGC) Stochastic Processes, Hidden Barriers.

be a partial differential equation (PDE). The dampening term $-\lambda \mathbf{v}$ constrains or limits the movement of the particle, as shown in Figure 1(b).

There are some unwanted complexities for our research in dealing with multiple particles, namely the interaction of every particle with its nearest neighbouring particles. Hence, we focus on the simpler case of a 1-Dimensional Itô diffusion.

Turning to Chemistry and Biochemistry, further more relevant examples of subtle constraining of a stochastic process include concentration gradients, in which a molecule diffuses within a medium which becomes increasingly more concentrated. In Biology, the diffusion of particles such as nutrients and minerals, through a porous membrane can become increasingly constrained the further they pass through the membrane. We note though that these various fields require numerous variables such as temprature, and so are too limited for our mathematical purposes.

Definition 1.1. Bi-Directional Grid Constrained (BGC) Stochastic Process. A BGC stochastic process for a random variable X over time t is one in which the further it departs from the origin, then the further it will be constrained from above and below (bi-directionally) along that X dimension.

This BGC defnition is expressed more precisely as an SDE in (3.12) and has been illustrated in Figure 1(a).

Before progressing further, it is important to define the use of two barriers per dimension of the Itô diffusion, as shown in Figure 2.

Figure 2 shows and as will become more apparent in the Methodology section that BGC is an 'infinitely scalable process' (i.e. can be generalized to higher dimensions) via the use of n-Dimensional Itô processes, but it will suffice for the purposes of this paper to revert to simply 1-Dimensional Itô processes. Whilst BGC involves more subtle barriers than these hard barriers, Figure 2 illustrates that two barriers are required per dimension for Bi-Directional Grid Constraining to occur, as every dimension of possible movement requires to be constrained above and below the origin. It is also worthwhile defining the types of barriers in Figure 3.

We now begin formalizing a 'first principles' approach to finding a mathematical expression for BGC, and one such approach could be to consider each equally spaced vertical level or graduation mark of Figure 4 to be rotated by 90°, to behave as a horizontal barrier in which the first barriers closest to the origin are fully transmissive barriers. As the Itô diffusion reaches the next horizontal barrier at some equally spaced interval Δx (hence the usage of 'grid' for $\mathbb{R}^{n\geq 2}$), then it becomes less transmissive and more reflective. Ultimately, there will be one uppermost and one lowermost barrier that will be fully reflective.

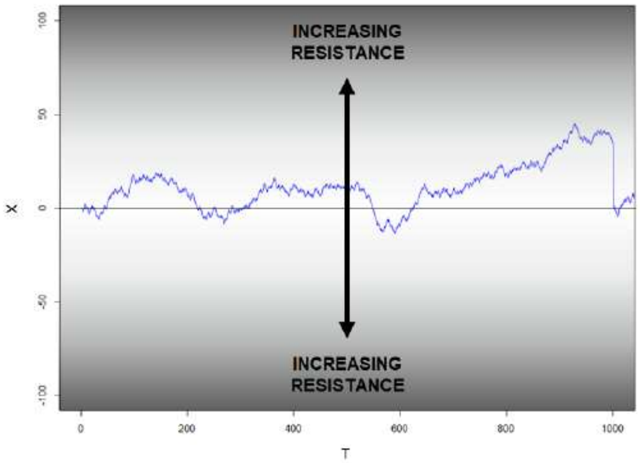

(a). Vertical Gradient(s) - (Bi-Directional)

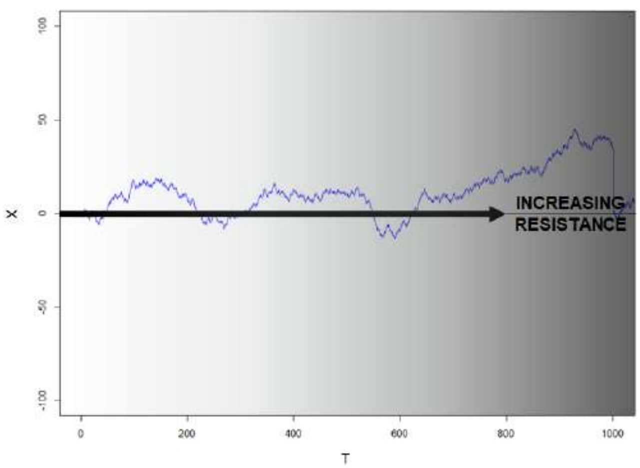

(b). Horizontal Gradient - (Uni-Directional)

FIGURE 1. Two Types of Incremental Gradients for Itô Diffusions
(a). Itô diffusion is constrained from above and below (bi-directionally), the more it vertically drifts away from the origin over time.
(b). Itô diffusion is constrained to the right (uni-directionally), the more it horizontally drifts away from the origin over time.

Let $\mathbb{P}(x, t)$ be the probability that the random variable X is at position x at time t. Then according to the rule of movement of the variable, there are only two possibilities that it reaches position x at time $t + \Delta t$. The variable was either at $x - \Delta x$ at time Δt and jumped to the right; or the variable was at $x + \Delta x$ at time Δt and jumped to the left as shown in Figure 4.

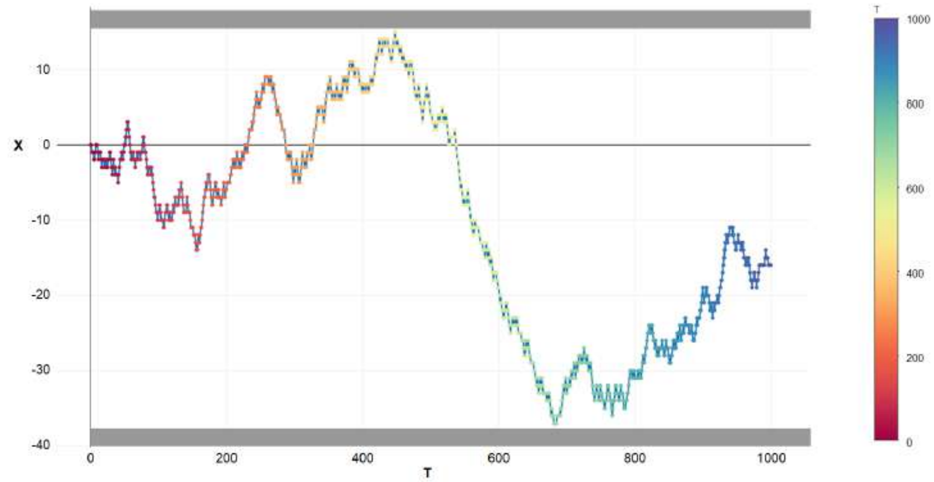

(a). Horizontal Reflective Barriers

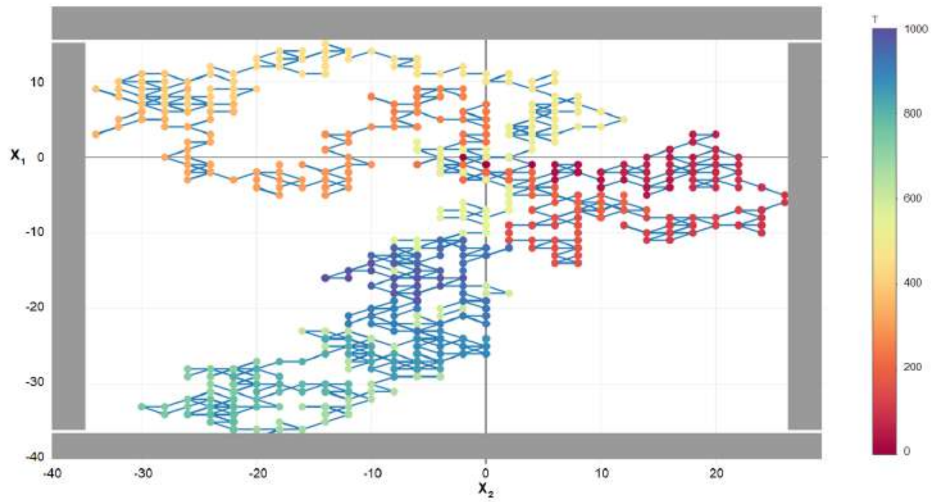

(b). Horizontal & Vertical Reflective Barriers

FIGURE 2. Barrier Orientation and Dimension of Itô Diffusions

As the Itô diffusions evolve over 1,000 time steps, we colorize each step according to its index in relation to the hot to cold colour scale.
(a). Colorization is not required (but still applied) as the time axis is explicit and so the evolution of the 1-Dimensional Itô diffusion is clear.
(b). Colorization helps visualise the evolution of the 2-Dimensional Itô diffusion over time, noting that we are now looking "top down" along the implicit time axis.

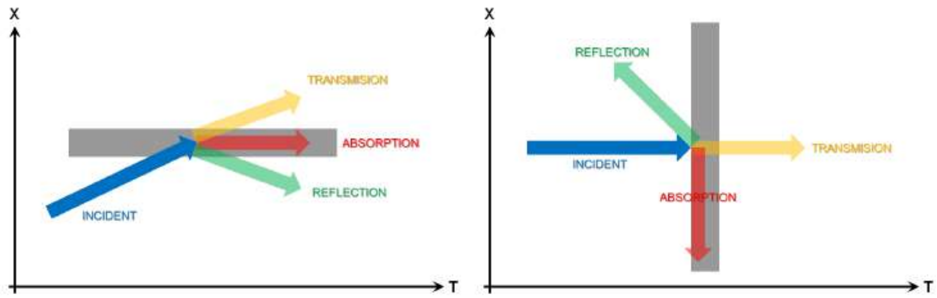

(a). Horizontal Barrier **(b). Vertical Barrier**

FIGURE 3. Three Main Types of Hard Barriers and Their Two Main Orientations

(a). The 1-Dimensional Itô diffusion can be used since the barrier is horizontal.
(b). The only way a reflection from a vertical barrier can occur is if an n-Dimensional Itô diffusion is used, where $n \geq 2$ (otherwise it would be travelling backwards in time).

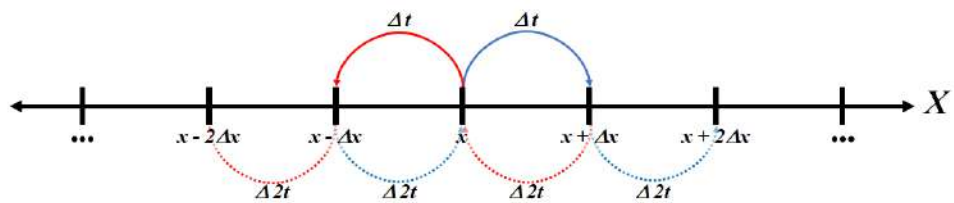

FIGURE 4. A Random Walk on a 1-Dimensional Lattice (Chain)
X = Distance , $t \in [0, T]$ = Time
Solid lines = $t + \Delta t$, Dotted lines = $t + 2\Delta t$

Since the next movement of the variable is independent of its present location, the probability that the variable is at position x at time $t + \Delta t$ given that it was at position $x - \Delta x$ at time t is $\frac{1}{2}\mathbb{P}(x - \Delta x, t)$, while the probability that the variable is at position x at time $t + \Delta t$ given that it was at $x + \Delta x$ at time t is $\frac{1}{2}\mathbb{P}(x + \Delta x, t)$. Thus, the probability that the variable is at a position at a point in time is given as follows for the first two cases.

At $t + \Delta t$:

$$\mathbb{P}(x, t + \Delta t) = \frac{1}{2}\mathbb{P}(x - \Delta x, t) + \frac{1}{2}\mathbb{P}(x + \Delta x, t).$$

At $t + 2\Delta t$:

$$\begin{aligned}\mathbb{P}(x, t + 2\Delta t) &= \frac{1}{2}\mathbb{P}(x - 2\Delta x, t) + \frac{1}{2}\mathbb{P}(x + 2\Delta x, t) \\ &\quad + \frac{1}{2}\mathbb{P}(x - \Delta x, t) + \frac{1}{2}\mathbb{P}(x + \Delta x, t).\end{aligned}$$

By proceeding in this manner, one can amass a series of difference equations, each for different time periods and then combine them, some having terms that cancel out, to derive the general equation. Khantha & Balakrishnan (1983) [8] and the references therein extend such an approach to have biassed random variables where the probability of moving to the left is not the same as the probability of moving to the right. These authors also introduce various barriers in the framework of lattices. However, this approach assumes that the direct constraining is due to either 100% absorptive barriers, 100% reflective barriers or 100% transmissive barriers. It would be much more difficult to formulate the subtle gradual constraining required for of BGC stochastic processes in the same lattice framework. We thus turn to Itô calculus for a more mathematically elegant approach to defining and assessing the true impact of BGC on stochastic processes.

When we examine numerous Itô diffusions, we know that a crude approximation of the paths' bounds is $\pm\sqrt{t}$. A far more accurate estimate for the upper and lower bounds is the Law of the Iterated Logarithm (LIL) in the formulation proved by Kolmogorov (1929) [10], which is referenced in the Literature Review and stated in the Methodology section. This is shown in Figure 5.

It is worthwhile noting that when we zoom into Figure 5, the LIL is undefined in $[0, e)$ and also that the LIL soon overtakes $\sqrt{t}$, as shown in Figure 6.

From Figure 6, the LIL can be ignored for $t \in [0, e)$ unless we make an adjustment by e to result in $\sqrt{2t\ln(\ln(t))} - e$.

We wish to quantify the impact of BGC on the LIL for a BGC Itô process but first we review the literature on this topic. In the Methodology section, we define the SDE of BGC in (3.12) as,

$$dX = \Big(f(X,t) - \text{sgn}[X,t]\lambda(X,t)\Big)\,dt + g(X,t)\,dW_t,$$

along with all its terms and prove the corresponding BGC theorem. The Results & Discussion section then adds visually beneficial simulations to further support our BGC theorem.

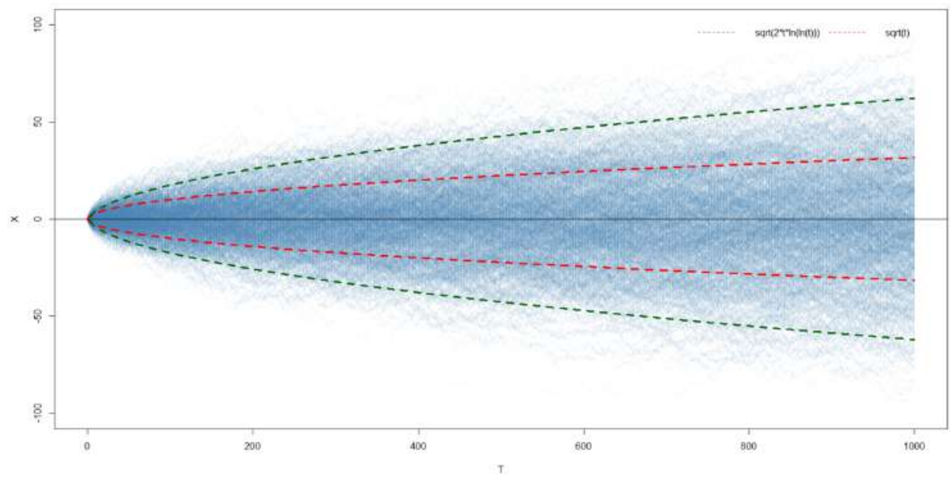

FIGURE 5. Law of Iterated Logarithm Simulated
Green envelope $= \sqrt{2t\ln(\ln(t))}$, **Red envelope** $= \sqrt{t}$.

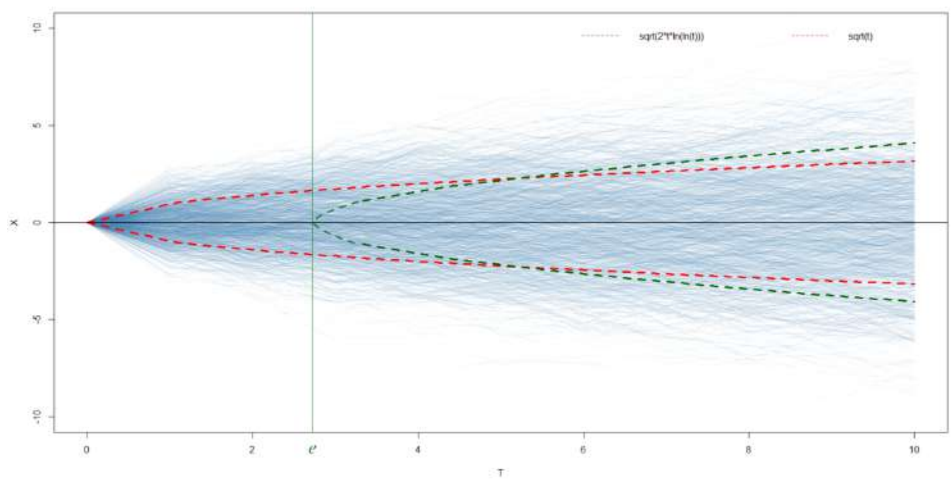

FIGURE 6. Law of Iterated Logarithm Simulated Zoomed
Green envelope $= \sqrt{2t\ln(\ln(t))}$, **Red envelope** $= \sqrt{t}$.

2. Literature Review

The original statement of the law of the iterated logarithm (LIL) is due to Khinchin (1924) [9] and was later restated and refined by Kolmogorov (1929) [10] and is stated in theorem 3.1. Since then, there has been a tremendous amount of work on the LIL for various kinds of random sequences and for stochastic processes. The following is a small sample of notable developments. Hartman & Wintner (1941) [6] generalized LIL to random walks with increments with zero mean and finite variance. Strassen (1964) [18] studied LIL from the point of view of invariance principles. Feller (1969) [5] examined limit theorems for the probabilities of large deviations. Stout (1970) [17] generalized the LIL to stationary ergodic martingales. Major (1977) [13] extended Feller's approach by proving a generalized version of Kolmogorov's LIL. De Acosta (1983) [4] gave a simple proof of the so-called 'Hartman-Wintner' version of LIL. Wittmann (1985) [24] generalized the 'Hartman-Wintner' version of LIL to random walks satisfying milder conditions. Vovk (1987) [23] derived a version of LIL valid for a single chaotic sequence. More recently, Berkes & Borda (2018) [3] proved the law of the iterated logarithm for $\sum_{k=1}^{N} \exp(2\pi i n_k \alpha)$ if the gaps $n_{k+1} - n_k$ are independent and identically distributed (iid) random variables. Krebs (2020) [11] examined the LIL and related strong invariance principles for functionals in stochastic geometry.

Despite these deep results in the application of real analysis to random variables, there was a gap in the literature when it comes to the application of LIL to to Itô diffusions until the 1950s. Tanaka (1958) [19] was one of the first to extend the LIL to one-dimensional diffusion processes. Motoo (1959) [16] then provided a proof of the LIL through the use of the diffusion equation. Mishra & Acharya (1983) [15] introduced normalization in the LIL of diffusions. Kawazu *et. al.* (1989) [7] extended the limit theorems for the asymptotic extremes of diffusions. Mao (2008) [14] simplified the previous research on LIL for diffusions and defined the paremeters ρ and L for a proof that extends to n-Dimensional diffusions. Finally, Appleby & Wu (2009) [2] provide a modern synthesis of the main research in LIL for diffusions by examining the solutions of SDEs that obey the LIL. They also provide application of these bounds to financial markets. Appleby & Appleby-Wu (2013) [1] then also examined recurrent solutions these SDEs that obey the LIL.

Having reviewed the literature of the LIL, the Methodology section formulates the novel impact that BGC has on the unconstrained LIL.

3. Methodology

Theorem 3.1. ***(Kolmogorov's Law of Iterated Logarithm (LIL)*** [10]***).*** *Let $X_1, X_2, \dots$ be independent and identically distributed (iid) random variables where $\mathbb{E}(X_i) = 0$, $\mathbb{E}(X_i^2) = \sigma_i^2$, $\forall i \in \mathbb{N}$. Define $S_n = \sum_{i=1}^{n} X_i$, $B_n = \sum_{i=1}^{n} \sigma_i^2$, $\forall i, n \in \mathbb{N}$ and let $B_n \to \infty$. Assume the existence of a numerical sequence M_n, $\forall i \in \mathbb{N}$ such that,*

$$M_n = \mathcal{O}\left(\sqrt{\frac{B_n}{\ln(\ln(B_n))}}\right) \quad , \quad \mathbb{P}\Big(|X_n| \leq M_n\Big) = 1.$$

Then the following relation is true,

$$\mathbb{P}\left(\limsup_{n\to\infty}\left\{\frac{S_n}{\sqrt{2B_n \ln(\ln(B_n))}}\right\} = 1\right) = 1.$$

The interested reader is invited to see the proof of this theorem, in its original Russian wording (Kolmogorov, 1929 [10]). The denominator of this infinite sequence is the envelope bounds as seen in Figure 5, whereas the numerator is of the random sequence S_n itself. The fact that the ratio approaches unity indicates that S_n is bounded above and below by the envelope. Such sequences are useful for Markov chains, martingales, Lévy processes and other theoretical topics regarding the asymptotic nature of random series. Instead, we wish to focus on the LIL for Itô processes, especially under BGC. We also use the natural logarithm $\ln(x)$ notation rather than the traditional $\log(x)$ used in the literature because $\log(x) = \log_\kappa(x)$ is usually reserved for κ=2 or 10, not for $\kappa = e$, which is what the literature is referring to.

Standard Brownian Motion (SBM) is defined as $dX = f(X,t)\,dt + g(X,t)\,dB_t$, and Geometric Brownian Motion (GBM) is defined as $dX = f(X)\,dt + g(X)\,dB_t$, where B_t is a Brownian process. However, Brownian motion does not have a drift term $f(X,t)$ but only a diffusion term $g(X,t)$ and we prefer to use the more mathematically precise Wiener process W_t definition instead of B_t. We thus define the following mutually exclusive terminology, in decreasing order of complexity.

Standard Itô Diffusion:

$$dX = f(X,t)\,dt + g(X,t)\,dW_t, \quad t \geq 0, \tag{3.1}$$

Geometric Itô Diffusion:

$$dX = f(X)\,dt + g(X)\,dW_t, \quad t \geq 0, \tag{3.2}$$

Geometric Brownian Motion / Geometric Wiener Process:

$$dX = g\,dW_t, \quad t \geq 0, \quad \text{i.e. } g(X,t) \Rightarrow g \in \mathbb{R}, \tag{3.3}$$

Standard Brownian Motion / (Standard) Wiener Process:

$$dX = dW_t, \quad t \geq 0, \quad \text{i.e. } g(X,t) \Rightarrow 1, \tag{3.4}$$

where, $f(x) : \mathbb{R} \to \mathbb{R}$, $g(x) : \mathbb{R} \to \mathbb{R}$, $\forall x \in \mathbb{R}$ and,

$$\lim_{x\to\infty} f(x) \to \mu \quad , \quad \lim_{x\to\infty} g(x) \to \sigma. \tag{3.5}$$

Depending on whether the generalized $f(x)$ and $g(x)$ are used, or whether the simplified μ and σ are used, then the resulting theorems will either have more complexity, or less complexity, respectively. Before presenting these theorems, we list some of the relationships between $f(x)$ and $g(x)$ that are examined in Appleby & Wu (2009),

$$f(x) = \mathcal{O}\Big(g^{-1}(x)\Big) \Longleftrightarrow \limsup_{t\to\infty} \big|f(t)\big|\big|g(t)\big| < \infty, \tag{3.6}$$

and $f(x)$ and $g(x)$ are further related by the scale function $s_c(x)$ and the speed measure $m(dx)$ of the SDE defined by,

$$s_c(x) = \int_c^x \exp\Bigg(-2\int_c^y \frac{f(z)}{g^2(z)}\,dz\Bigg)\,dy, \quad m(dx) = \frac{2}{s'(x)g^2(x)}\,dx, \tag{3.7}$$

$c, x \in I := (l, r)$ respectively, where I is the state space of the process. The next theorem can now address the 'geometric' Itô diffusions of (3.2).

Theorem 3.2. *(Motoo, 1959). Let X be the unique continuous real-valued process satisfying the autonomous SDE as defined in (3.2) with $X(0) = x_0$. Let s and m be the scale function and speed measure of X as defined in (3.7), and let $h : (0,\infty) \to (0,\infty)$ be an increasing function with $h(t) \to \infty$ as $t \to \infty$. If X is recurrent on (l,∞) (or $[l,\infty)$ in the case when l is an instantaneous reflecting point) and $m(l,\infty) < \infty$, then,*

$$\mathbb{P}\Bigg[\limsup_{t\to\infty} \frac{|W(t)|}{\sqrt{2t\ \ln(\ln(t))}} \geq 1\Bigg] = 1 \ \textit{or}\ 0,$$

depending on whether,

$$\int_{t_0}^{\infty} \frac{1}{s(h(t))}\,dt = \infty, \ \textit{or}\ \int_{t_0}^{\infty} \frac{1}{s(h(t))}\,dt < \infty, \ \textit{respectively},$$

for some $t_0 > 0$. ∎

Mao (2008) extends Motoo's work by defining the terms ρ and K as,

$$xf(x) < \rho, \quad \big|\big|g(x,t)\big|\big| \leq K,$$

where by '$\leq$', it is meant that *most* $X(t)$ paths will not exceed these bounds, but some will as shown in Figure 5. Mao then proves the corresponding LIL,

$$\limsup_{t\to\infty} \frac{|X(t)|}{\sqrt{2t\ \ln(\ln(t))}} = K\sqrt{e} \quad a.s.,$$

with,

$$\lim_{x\to-\infty} xf(x) = L_{-\infty} > \frac{\sigma^2}{2},$$

and,

$$\lim_{x\to\infty} \frac{xf(x)}{g^2(x)} = L_{\infty} > \frac{1}{2}.$$

Note that $L_\infty < \infty$ as $x \to \infty$ when $f(x)$ and $g(x)$ are regularly varying at infinity. Mao's findings add greater understanding on the relationship between $f(x)$ and $g(x)$ but it is not an exact bound(s), and so the following theorem addresses the 'geometric' Itô diffusions of (3.2) more precisely than Motoo's theorem.

Theorem 3.3. *(Appleby & Wu, 2009, p.928). Let X be the unique continuous adapted process which obeys (3.2). Let $\Omega := \{\omega : \lim_{t\to\infty} X(t,\omega) = \infty\}$. If,*

$$\lim_{x\to\infty} xf(x) = L_\infty, \quad g(x) = \sigma, \tag{3.8}$$

where $x \in \mathbb{R}$, $\sigma \neq 0$ and $L_\infty > \sigma^2/2$, then $\mathbb{P}[\Omega] > 0$ and X satisfies,

$$\limsup_{t\to\infty} \frac{|X(t)|}{\sqrt{2t\,\ln(\ln(t))}} = |\sigma| \quad a.s.\ on\ \Omega, \tag{3.9}$$

and,

$$\liminf_{t\to\infty} \frac{\ln\left(\frac{X(t)}{\sqrt{t}}\right)}{\ln(\ln(t))} = -\frac{1}{\frac{2L_\infty}{\sigma^2} - 1} \quad a.s.\ on\ \Omega. \tag{3.10}$$

■

Finally, the following theorem by the same authors extends their previous theorem to 'standard' Itô diffusions of (3.1).

Theorem 3.4. *(Appleby & Wu, 2009, p.932). Let X be the unique continuous adapted process which obeys (3.2). Let $\Omega := \{\omega : \lim_{t\to\infty} X(t,\omega) = \infty\}$. If there exist positive real numbers L_∞ and σ such that $L_\infty > \sigma^2/2$, $f(x)$ obeys (3.8), and $g(x)$ obeys,*

$$\forall x \in \mathbb{R}, \quad g(x) \neq 0, \quad \lim_{x\to\infty} g(x) = \sigma \in \mathbb{R}_+, \tag{3.11}$$

then X satisfies (3.9) and (3.10).

Having reviewed all the current research that relates $f(x)$ and $g(x)$ in the most time dependent setting of (X,t), we now define the SDE of BGC stochastic processes.

Definition 3.5. (SDE of BGC Stochastic Process). For a complete filtered probability space $(\Omega, \mathcal{F}, \{\mathcal{F}\}_{t\geq 0}, \mathbb{P})$ and a BGC function $\Psi(x) : \mathbb{R} \to \mathbb{R}$, $\forall x \in \mathbb{R}$, then the corresponding BGC Itô diffusion is expressed as,

$$\begin{aligned} dX &= \Big(f(X,t)\,dt + g(X,t)\,dW_t\Big) - \operatorname{sgn}\Big[f(X,t)\,dt + g(X,t)\,dW_t\Big]\Psi(X,t)\,dt \\ &= \Big(f(X,t)\,dt + g(X,t)\,dW_t\Big) - \operatorname{sgn}[X,t]\Psi(X,t)\,dt \\ &= \Big(f(X,t) - \operatorname{sgn}[X,t]\Psi(X,t)\Big)\,dt + g(X,t)\,dW_t, \end{aligned} \tag{3.12}$$

where $\operatorname{sgn}[x]$ is defined in the usual sense as,

$$\operatorname{sgn}[x] = \begin{cases} 1 & , \quad x > 0 \\ 0 & , \quad x = 0\,, \\ -1 & , \quad x < 0 \end{cases}$$

and $f(X,t)$ and $g(X,t)$ are convex functions.

Now, the unconstrained stochastic process $X(t)$ is bounded by,

$$-\sqrt{2t\,\ln(\ln(t))} \leq X(t) \leq \sqrt{2t\,\ln(\ln(t))}.$$

At a high level, the BGC stochastic process $\overline{X(t)}$ is bounded by either,

$$-\sqrt{2t\,\ln(\ln(t))} + \Phi(t) \leq \overline{X(t)} \leq \sqrt{2t\,\ln(\ln(t))} - \Phi(t),$$

for some function $\Phi(t)$ or by,

$$-\Gamma(t) \leq \overline{X(t)} \leq \Gamma(t),$$

for some other function $\Gamma(t)$ where,

$$\big|\Gamma(t)\big| \leq \big|\sqrt{2t\,\ln(\ln(t))} + \Phi(t)\big|.$$

We will thus need to derive either $\Phi(t)$ or $\Gamma(t)$. The simplest possible theorem for BGC is to derive a new theorem from theorem 3.4.

Theorem 3.6. ***(BGC Mapping for LIL)***. *Let $X(t)$ be the unique continuous adapted process which obeys (3.2) and $\overline{X(t)}$ be the corresponding BGC process. If there exist positive real numbers L_∞ and σ such that $L_\infty > \sigma^2/2$, $f(x)$ obeys (3.8) and $g(x)$ obeys (3.11), then defining $F(x)$ and $G(x)$ as BGC versions of $f(x)$ and $g(x)$ as,*

$$F(x) := f(x) - \operatorname{sgn}[x]\Psi(x), \quad G(x) := g(x) - \operatorname{sgn}[x]\Psi(x), \tag{3.13}$$

where,

$$F(x) : \mathbb{R} \to \mathbb{R}, \quad G(x) : \mathbb{R} \to \mathbb{R}, \quad \forall x \in \mathbb{R}, \tag{3.14}$$

implies that $\overline{X(t)}$ also satisfies (3.9) and (3.10).

Proof. In general, for linear combinations of drift functions $f_i(x)$ and diffusion functions $g_j(x)$ respectively, $\forall a_i, b_j, n, m \in \mathbb{N}$, then,

$$\begin{array}{rcl} a_1 f_1(x) + \cdots + a_n f_n(x) & = & f_{n+1}(x) \\ b_1 g_1(x) + \cdots + b_m g_m(x) & = & g_{m+1}(x) \end{array},$$

are also drift and diffusion functions respectively. However, one can not simply end here since, after some minor abuse of notation, at sucessive time instances,

$$\begin{array}{rcl} X_1 & = & \Big(f(X_0) - \underbrace{\operatorname{sgn}[X_0]}_{\text{Impacts } X_1} \underbrace{\Psi(X_0)}_{\text{Impacts } X_1} \Big)\, dt + g(X_0)\, dW_0, \\ X_2 & = & \underbrace{\Big(f(X_1) - \operatorname{sgn}[X_1]\Psi(X_1) \Big)}_{\text{Impacts } X_2} dt + \underbrace{g(X_1)}_{\text{Impacts } X_2} dW_1, \\ \cdots & \cdots & \cdots \end{array}$$

shows that where BGC initially is acting on the drift at $t = 0$, it then impacts the diffusion (and drift) at $t = 1$, and so on, due the the iterative nature of Itô diffusions. This means our proof must not only consider the impact of BGC on $f(x)$ but also on $g(x)$. Now, (3.13) is true for the trivial case if $\operatorname{sgn}[x] = 1$ (i.e. there is no sign oscillation or sign switching). In all other cases of $\operatorname{sgn}[x]$, as the BGC Itô process $\overline{X(t)}$ oscillates above and below the $X = 0$ axis, it simply requires us to state that,

$$F(x) : \mathbb{R}_- \cup \mathbb{R}_+ \to \mathbb{R}, \quad G(x) : \mathbb{R}_- \cup \mathbb{R}_+ \to \mathbb{R}. \tag{3.15}$$

The only step remaining is to show that $F(x)$ and $G(x)$ guarantee that there exists a unique global continuous solution to the BGC SDE by verifying that these functions satisfy Lipschitz local continuity . The Lipschitz local continuity condition is satisfied if there exists a positive real constant Λ_1 such that $\forall x_1, x_2 \in \mathbb{R}$,

$$\begin{aligned}\big|F(x_1,t)-F(x_2,t)\big| &\leq \Lambda_1\big|x_1-x_2\big|, \quad t\geq 0,\\ \big|G(x_1,t)-G(x_2,t)\big| &\leq \Lambda_1\big|x_1-x_2\big|, \quad t\geq 0.\end{aligned}$$

Substituting (3.15) for $f(x)$ and $g(x)$ into theorem 3.4 completes the proof. □

For $F(x)$ and $G(x)$ to guarantee that there exists a unique ***strong*** global continuous solution to the BGC SDE, we would also need to establish that the Linear growth bound condition is satisfied, which is met if there exists a positive real constant Λ_2 such that $\forall x \in \mathbb{R}$,

$$\big|F(x,t)\big|^2+\big|G(x,t)\big|^2 \leq \Lambda_2\Big(1+\big|x\big|^2\Big), \quad t\geq 0, \tag{3.16}$$

which is dependent on the actual nature of $\Psi(X,t)$. If $\Psi(X,t)$ does not satisfy this condition, then the solution might explode in finite time.

4. Results and Discussion

To compliment the Methodology section, $\Psi(X,t)$ in (3.12) was instantiated in this Results section to be $\Psi(X,t) := \frac{x^2}{\beta}$, where $\beta = 100$ and $x \in \mathbb{R}$, as the simplest form of BGC stochastic processes, so that a geometric context can be provided. (3.12) was simulated over 1,000 time steps in Figure 7 for with and without BGC for various values of μ and σ. We note that whilst μ and σ are used here instead of the more general $f(X,t)$ and $g(X,t)$, we have actually catered for this by using $\Psi(X,t)$ rather than the autonomous constant Ψ.

From Figure 7, we can see in four different scenarios how BGC constrains the blue unconstrained Itô process into the constrained red Itô process, pulling it back the further it deviates from the origin in either extreme of X.

To extend this analysis further, (3.12) was simulated over 1,000 time steps for a total of 1,000 paths and is shown in Figure 8 with positive, zero, negative drift and with varying diffusion values.

From Figure 8, we see that most noticably in (d), that there are 'gaps'. To show this discretization in further detail, we reduced the marker size, not included the lines that connect the markers and increased their transparency. One can also see that the discretization polarizes the markers along the direction of the drift. To elaborate on this hidden barrier discretization phenomenon further, the densities of the simulations, before and after BGC were plotted in Figure 9.

From Figure 9, we see that the hidden barrier becomes obvious due to the vertical peak(s) suddenly dropping to zero. We also see some "sinusoidal" accumulations, especially in (a) and (b), which correlate with the discrete bands in Figure 8. Even if the minima of these peaks are non-zero, due to the transparency feature of Figure 8, the relative colouring can imply that BGC causes regions where there

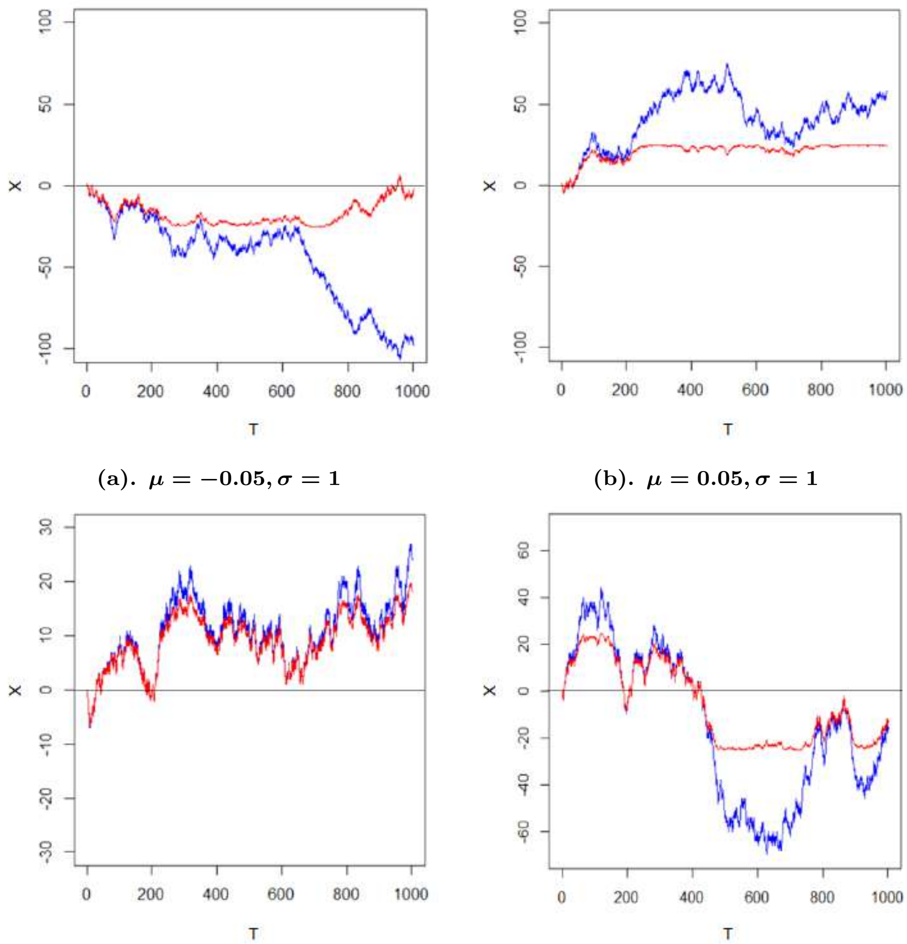

(a). $\mu = -0.05, \sigma = 1$ **(b). $\mu = 0.05, \sigma = 1$**

(c). $\mu = 0, \sigma = 1$ **(d). $\mu = 0, \sigma = 2$**

FIGURE 7. 4 Simulations of 1,000-Step 1-Dimensional Itô Diffusions, With & Without BGC

Blue = Without BGC , Red = With BGC

(a). *Negative* μ shows most constraining occurs the *lower* X_t moves from origin.
(b). *Positive* μ shows most constraining occurs the *higher* X_t moves from origin.
(c). *Small* σ shows most constraining occurs the further X_t moves from origin.
(d). *Larger* σ shows most constraining occurs the further X_t moves along X.

are no simulation path values, even though some values that are represented or detected.

Having held mainly σ insignificant by setting $\sigma = 1$ whilst varying μ, we now hold μ to be insignificant by setting $\mu = 0$ whilst varying σ, as shown in Figure 10.

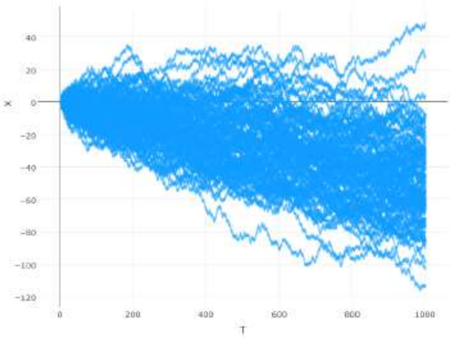

(a). $\mu = -0.05, \sigma = 1$ without BGC

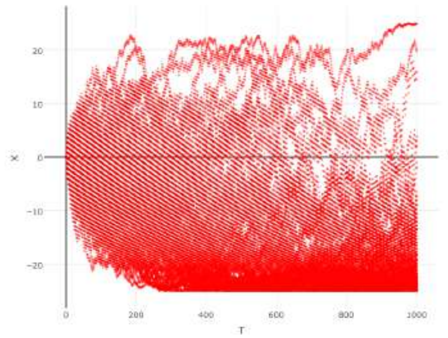

(b). $\mu = -0.05, \sigma = 1$ with BGC

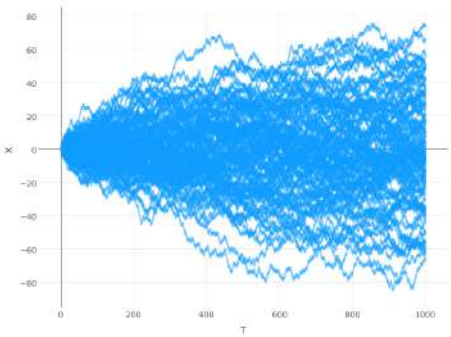

(c). $\mu = 0, \sigma = 1$ without BGC

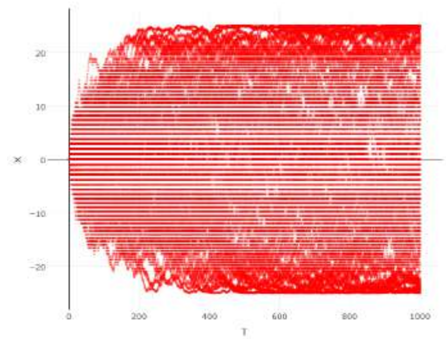

(d). $\mu = 0, \sigma = 1$ with BGC

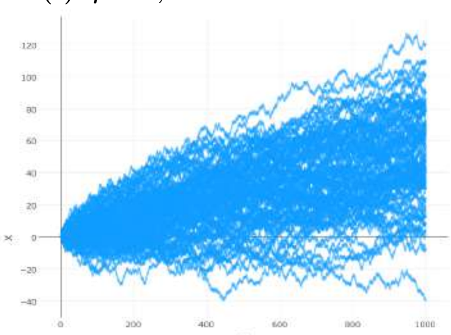

(e). $\mu = 0.05, \sigma = 1$ without BGC

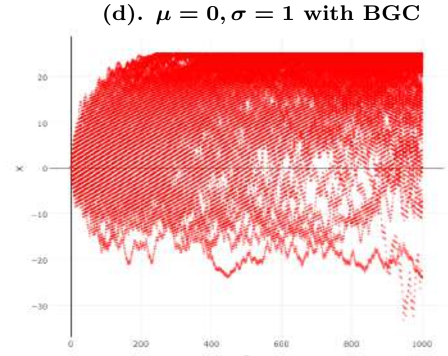

(f). $\mu = 0.05, \sigma = 1$ with BGC

FIGURE 8. Discretization Details of Simulations due to BGC with no Diffusion

(a). *Negative* drift is constrained in (b) the more it deviates away from the origin, causing *downward* diagonal bands to form.
(c). *Zero* drift is constrained in (d) the more it deviates away from the origin, causing horizontal bands to form.
(e). *Positive* drift is constrained in (f) the more it deviates away from the origin, causing *upward* diagonal bands to form.
(b), (d) & (f): Exponentially 'attracted' to hidden horizontal (reflective) barrier(s).

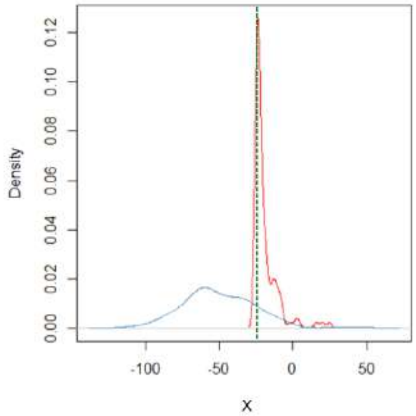

(a). $\boldsymbol{\mu = -0.05, \sigma = 1}$

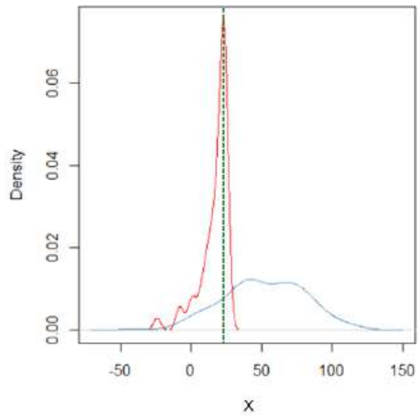

(b). $\boldsymbol{\mu = 0.05, \sigma = 1}$

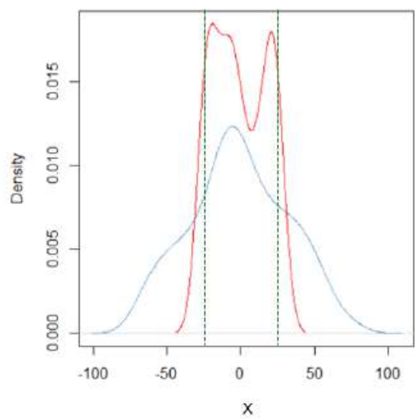

(c). $\boldsymbol{\mu = 0, \sigma = 1}$

FIGURE 9. Impact of BGC on the Distribution of Itô Diffusions with no Diffusion Term

Blue = original density , Red = BGC density , Green = peak.

(a). BGC squeezes the *negative* skew distribution to *positive* direction due to impact of hidden BGC barrier.
(b). BGC squeezes the *positive* skew distribution to the *negative* direction due to impact of hidden BGC barrier.
(c). BGC squeezes the *zero* skew distribution to both the *negative* and *positive* direction due to impact of hidden BGC barrier.
Notice the 'sinusoidal' nature of BGC distributions, which was being exhibited in Figure 8 as banding or discretization.

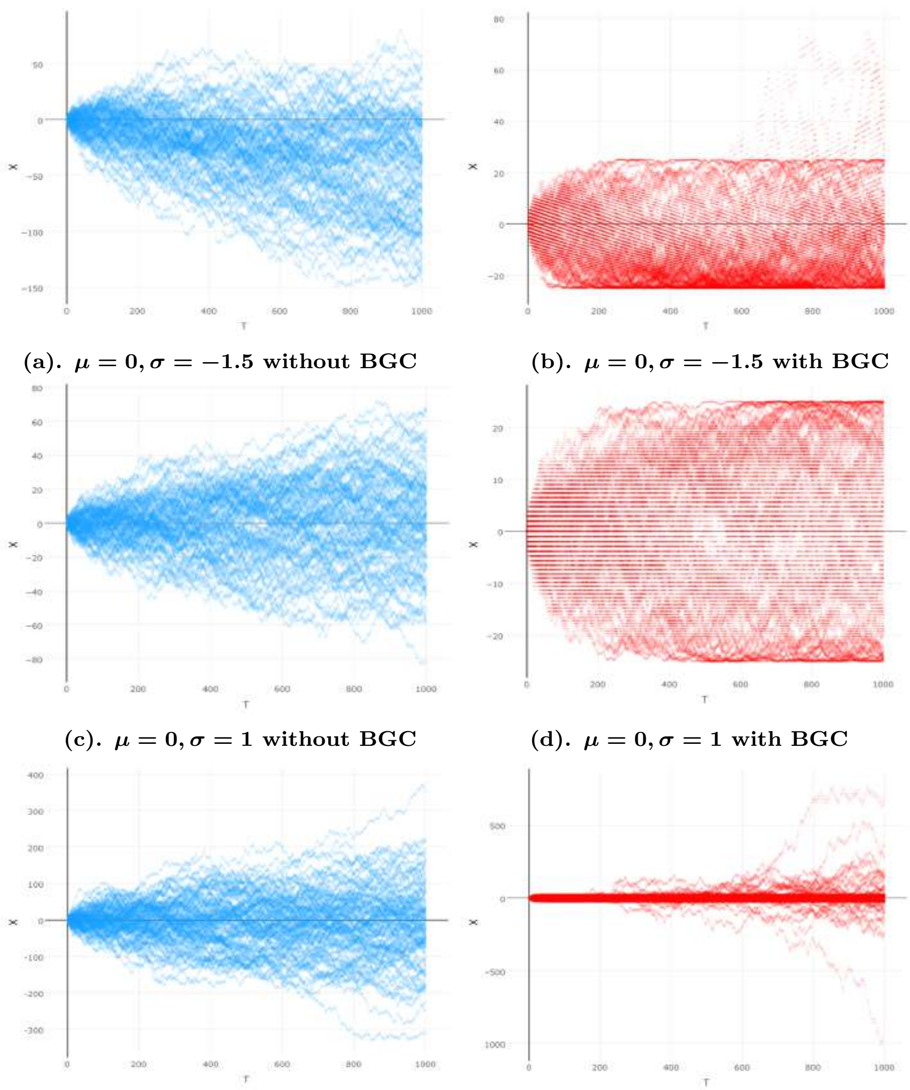

(a). $\mu = 0, \sigma = -1.5$ **without BGC**

(b). $\mu = 0, \sigma = -1.5$ **with BGC**

(c). $\mu = 0, \sigma = 1$ **without BGC**

(d). $\mu = 0, \sigma = 1$ **with BGC**

(e). $\mu = 0, \sigma = 3.5$ **without BGC**

(f). $\mu = 0, \sigma = 3.5$ **with BGC**

FIGURE 10. Discretization Details of Simulations due to BGC with no Drift

(a). ***Negative*** **diffusion is constrained in (b) the more it deviates away from the origin, causing** ***downward*** **diagonal bands to form, with** ***some*** **Itô diffusions escaping the hidden reflective barrier since σ's effect is** ***overtaken.***
(c). ***Neutral*** **diffusion is constrained in (d) the more it deviates away from the origin, causing horizontal bands to form, with** ***no*** **Itô diffusions escaping the hidden reflective barrier since σ's impact is the** ***smallest.***
(e). ***Positive*** **diffusion is constrained in (f) the more it deviates away from the origin, causing** ***upward*** **diagonal bands to form, with** ***some*** **Itô diffusions escaping the hidden reflective barrier since σ's effect is** ***overtaken.***

We also note that in (b), (d) and (f), the transitions are exponentially 'attracted' to the hidden (reflective) barrier.

From Figure 10, we can see that the BGC constrains the Itô diffusions in the similar way as Figure 8, but as time continues to increase (or pass), then the impact of BGC diminishes. This means that the reflective barrier nature of BGC becomes overtaken by the Itô process itself when the magnitude of σ forces the process to escape the barrier.

To statistically assess the impact of BGC on the resulting distributions, the corresponding densities were plotted in Figure 11, the most noticable being (b).

5. Conclusions

This paper has introduced the novel theory of Bi-Directional Grid Constrained (BGC) stochastic processes, where the further an Itô diffusion drifts away from the origin, then the more it will be constrained. The net effect of the BGC operates as a reflecting horizontal hidden barrier, from which we derived a theorem for the logarithmic bounds of the resulting envelope. We have also shown how BGC effectively discretizes the Itô diffusion paths into discrete bands, which is surprising. We have also shown that if the diffusion parameter σ is relatively large in comparison to the BGC $\Psi(X,t)$ function's magnitude, then the Itô diffusions can escape or be transmitted from the hidden barrier. These results are infinitely scalable to n-Dimensional Itô diffusions, although the proof of which is reserved for future research.

There are immediate applications of this research, not only in finance (Taranto & Khan, 2020) [20], [21], [22], but also in many other fields. Due to our Itô process formulation, without requiring the typically high amount of parameters found in fields such as Physics and Economics, we find that our formulation supports greater portability to many fields. One such typical application of BGC can be in the monetary policies of increasing quantitative easing as it can reduce or constrain the growth of unemployment or alternatively the growth of inflation, but after some time, the stimulus can end up having little or no effect (or worse, have an adverse effect). It can also polarize or discretize the associated Itô process that it is trying to constrain, such as displacing or marginalizing individuals or groups of individuals. Future research on this topic can include the geometric classification of BGC functions and the estimation of the first passage time (FPT) for when the resulting BGC hidden barrier is hit.

References

1. Appleby J., Appleby-Wu H. (2013). Recurrent solutions of stochastic differential equations with non-constant diffusion coefficients which obey the law of the iterated logarithm. arXiv preprint arXiv:1310.2629.
2. Appleby J., Wu H. (2009). Solutions of stochastic differential equations obeying the law of the iterated logarithm, with applications to financial markets. *Electronic Journal of Probability*, 14, pp.912-959.
3. Berkes I., Borda B. (2019). On the Law of the Iterated Logarithm for Random Exponential Sums. *Transactions of the American Mathematical Society*, 371(5), pp.3259-3280.

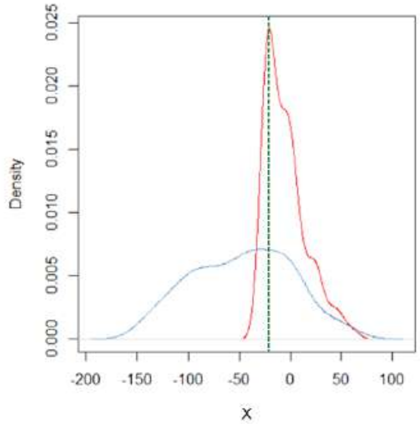

(a). $\mu = 0, \sigma = -1.5$

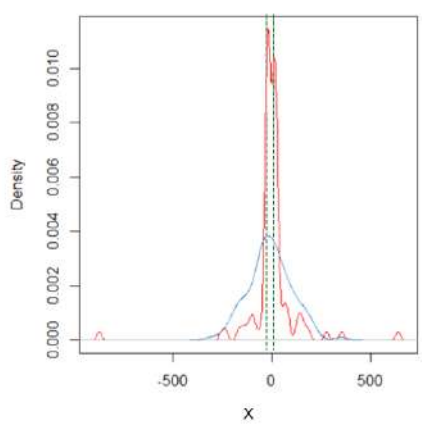

(b). $\mu = 0, \sigma = 3.5$

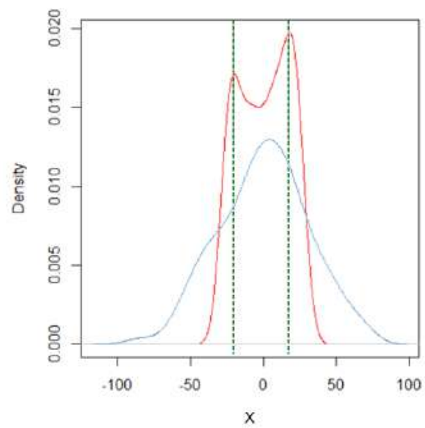

(c). $\mu = 0, \sigma = 1$

FIGURE 11. Impact of BGC on the Diffusion Altered Distribution of Itô Diffusions

Blue = original density , Red = BGC density , Green = peak.

(a). BGC squeezes the *negative* skew distribution to the *positive* direction due to the impact of the hidden BGC barrier.

(b). BGC squeezes the *positive* skew distribution to the *negative* direction due to the impact of the hidden BGC barrier.

(c). BGC squeezes the *zero* skew distribution to both the *negative* and *positive* direction due to the impact of the hidden BGC barrier.

4. de Acosta A. (1983). A new proof of the Hartman-Wintner Law of the Iterated Logarithm. *The Annals of Probability*, 11(2), pp.270-276.
5. Feller W. (1969). Limit Theorems for Probabilities of Large Deviations. *Z. Wahrscheinlichkeitstheorie verw. Gebiete*, 14, p.1-20.
6. Hartman P., Wintner A. (1941). On the Law of the Iterated Logarithm. *American Journal of Mathematics*, 63(1), pp.169-176.

7. Kawazu K., Tamura Y. & Tanaka H. (1989). Limit theorems for one-dimensional diffusions and random walks in random environments. *Probability Theory and Related Fields*, 80(4), pp.501-541.
8. Khantha M., Balakrishnan V. (1983). First passage time distributions for finite one-dimensional random walks. *Pramana*, 21(2), pp.111-122.
9. Khinchine A. (1924). Über einen Satz der Wahrscheinlichkeitsrechnung. *Fundamenta Mathematicae* 6: pp. 9–20.
10. Kolmogorov A. (1929). Ueber das Gesetz des Iterierten Logarithmus. *Math. Ann.*, Vol. 101, p.126-135.
11. Krebs J. (2020). On the Law of the Iterated Logarithm and Strong Invariance Principles in Computational Geometry. *Preprint sourced from arXiv* https://arxiv.org/abs/2002.09764
12. Langevin P. (1908). Sur la Théorie du Mouvement Brownien. *Comptes rendus de l'Académie des Sciences.* 146: 530–533.
13. Major P. (1977). A Note on Kolmogorov's Law of Iterated Logarithm. *Studia Scientiarum Mathematicarum Hungarica*, Vol. 12, p.161-167.
14. Mao X. (2008). *Stochastic Differential Equations and Applications.* Second edition. Horwood Publishing Limited, Chichester, Math. Review 2009e;60004. MR2380366.
15. Mishra M., Acharya S. (1983). On normalization in the law of the iterated logarithm for diffusion processes. *Indian Journal of Pure and Applied Mathematics*, 14(11): 1335-1342.
16. Motoo M. (1959). Proof of the law of iterated logarithm through diffusion equation. *Annals of the Institute of Statistical Mathematics* 10, 21–28. https://doi.org/10.1007/BF02883984.
17. Stout W. (1970). The Hartman-Wintner Law of the Iterated Logarithm for Martingales. *The Annals of Mathematical Statistics*, 41(6), pp.2158-2160.
18. Strassen V. (1964). An Invariance Principle for the Law of Iterated Logarithm. *Z. Wahrscheinlichkeitstheorie verw. Gebiete*, 3, p.211-226.
19. Tanaka H. (1958). Certain limit theorems concerning one-dimensional diffusion processes. *Memoirs of the Faculty of Science, Kyushu University.* Series A, Mathematics, 12(1), pp.1-11.
20. Taranto A. and Khan, S. (2020). Gambler's ruin problem and bi-directional grid constrained trading and investment strategies. *Investment Management and Financial Innovations*, 17(3), pp.54-66.
21. Taranto A. and Khan, S. (2020). Bi-directional grid absorption barrier constrained stochastic processes with applications in finance and investment. *Risk Governance & Control: Financial Markets & Institutions*, 10(3), pp.20-33.
22. Taranto A. and Khan S. (2020). Drawdown and Drawup of Bi-Directional Grid Constrained Stochastic Processes. *Journal of Mathematics and Statistics*, 16(1), pp.182-197.
23. Vovk V. (1987). Law of the Iterated Logarithm for Kolmogorov Random–or Chaotic–Sequences. *Teoriya Veroyatnostei i ee Primeneniya*, 32(3), pp.456-468.
24. Wittmann R. (1985). A General Law of Iterated Logarithm. *Zeitschrift für Wahrscheinlichkeitstheorie und Verwandte Gebiete*, 68(4), pp.521-543.

The first author was supported by an Australian Government Research Training Program (RTP) Scholarship.

We would like to thank Prof. Laura Sacerdote of Università Degli Studi Di Torino, for her invaluable advice on refining the early stages of the paper. We would also like to thank the independent referees of this journal for their endorsements and suggestions.